Nanoscale

Accepted Manuscript

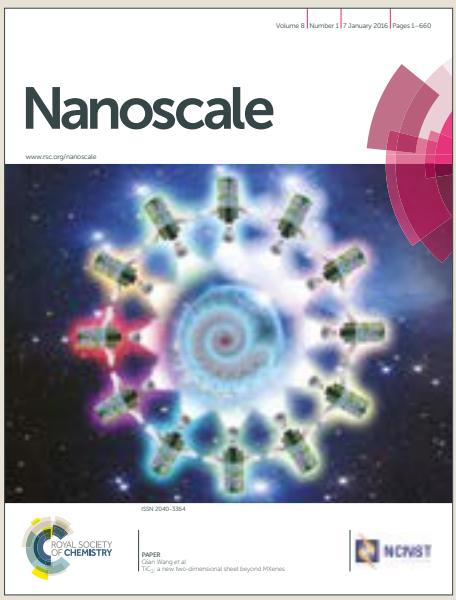

This is an Accepted Manuscript, which has been through the Royal Society of Chemistry peer review process and has been accepted for publication.

Accepted Manuscripts are published online shortly after acceptance, before technical editing, formatting and proof reading. Using this free service, authors can make their results available to the community, in citable form, before we publish the edited article. We will replace this Accepted Manuscript with the edited and formatted Advance Article as soon as it is available.

You can find more information about Accepted Manuscripts in the author guidelines.

Please note that technical editing may introduce minor changes to the text and/or graphics, which may alter content. The journal's standard Terms & Conditions and the ethical guidelines, outlined in our author and reviewer resource centre, still apply. In no event shall the Royal Society of Chemistry be held responsible for any errors or omissions in this Accepted Manuscript or any consequences arising from the use of any information it contains.

ROYAL SOCIETY OF CHEMISTRY

rsc.li/nanoscale

Journal Name

ARTICLE

Tuning contact conductance of anchoring groups in single molecule junctions by molecular design

Received 00th January 20xx,
Accepted 00th January 20xx

DOI: 10.1039/x0xx00000x

www.rsc.org/

Jakub Šebera,[a] Marcin Lindner,[b†] Jindřich Gasior,[a] Gábor Meszáros,[c] Olaf Fuhr,[b] Marcel Mayor,[b,d] Michal Valášek,*[b] Viliam Kolivoška,*[a] and Magdaléna Hromadová*[a]

Tetraphenylmethane tripod functionalized with three thiol moieties in *para* position can serve as a supporting platform for functional molecular electronic elements. A combined experimental scanning tunneling microscopy break junction technique with theoretical approaches based on density functional theory and non-equilibrium Green's function formalism were used for detailed charge transport analysis to find configurations, geometries and charge transport pathways in molecular junctions of single molecule oligo-1,4-phenylene conductors containing this tripodal anchoring group. The effect of molecular length (n = 1 to 4 repeating phenylene units) on the charge transport properties and junction configurations is addressed. The number of covalent attachments between the electrode and the tripodal platform changes with n affecting the contact conductance of the junction. The longest homologue n = 4 adopts an upright configuration with all three *para* thiolate moieties of the tripod attached to the gold electrode. Contact conductance of the tetraphenylmethane tripod substituted by thiols in *para* position is higher than of that substituted in *meta* position. Such molecular arrangement is highly conducting and allows well-defined directional positioning of a variety of functional groups.

Introduction

Molecular electronics aims at realizing functional electronic devices relying on molecular building blocks. A robust and directional contact between molecular components and a metallic electrode is viewed as an essential prerequisite to fabricate well-defined architectures for molecular electronic applications. Multipodal platforms were developed recently to establish a directional attachment of molecules to metallic surfaces.[1,2] Tripodal scaffolds are their most common representatives and include triazatriangulene,[3–5] trioxatriangulene,[6] cyclohexane trithiol,[7] adamantane,[8–11] tris(azobenzyl)amine,[12] spirobifluorene,[13–16] tetraphenylmethane[17–22] and tetraphenylsilane[23,24] moieties.

The principal function of molecular electronic components is the transport of electric charge. The latter may be investigated at the single molecule level by various approaches including scanning tunneling microscopy break junction (STM-BJ) technique.[25] Charge transport properties of single molecule electronic components based on tripodal platforms were investigated in several recent contributions focusing on elucidation of charge transport mechanism[3,21,24] and analysis of molecular junction (MJ) geometries.[14–16,21,22] Theoretical analysis of the charge transport in MJs used the combination of density functional theory (DFT) and non-equilibrium Green´s function (NEGF) formalism. Further, the DFT/NEGF approach was successfully employed to examine the charge transport in molecular electronic elements supported by tripodal platforms including triazatriangulene,[3] adamantane,[11] spirobifluorene[14-16] and tetraphenylmethane[19,21] moieties.

Tetraphenylmethane moiety possessing three thiol groups as anchors has recently attracted considerable attention as a potential platform to support molecular electronic components.[17,18,21,22] Molecular conductors based on this platform possessing 1,4-phenylene as a repeating unit in the principal molecular backbone capped with the –CN moiety were found to show unique behavior when chemisorbed on the Au(111) surface. At cryogenic temperatures, high-resolution STM imaging revealed that self-assembled monolayers are formed with molecules lying parallel to the surface.[17] At ambient temperature, electrochemical reductive desorption experiments combined with DFT molecular modeling revealed that the same conductors form densely packed self-assembled monolayers with molecules standing upright on the Au(111) surface with all three thiolate moieties being involved in the covalent attachment to the surface.[21] STM-BJ measurements further discovered that molecules form highly conductive single MJs in which the electric charge is

[a] J. Heyrovský Institute of Physical Chemistry of the CAS, v.v.i., Dolejškova 3, 18223 Prague, Czech Republic. E-mail: hromadom@jh-inst.cas.cz, viliam.kolivoska@jh-inst.cas.cz
[b] Karlsruhe Institute of Technology (KIT), Institute of Nanotechnology, P. O. Box 3640, 76021 Karlsruhe, Germany. E-mail: michal.valasek@kit.edu
[c] Research Centre for Natural Sciences, HAS, Magyar tudósok krt. 2, H-1117 Budapest, Hungary.
[d] Department of Chemistry, University of Basel, St. Johanns-Ring 19, 4056 Basel, Switzerland.
† Present address: Institute of Organic Chemistry, Polish Academy of Sciences, Kasprzaka 44/52, 01-224 Warsaw, Poland
Electronic Supplementary Information (ESI) available: [details of any supplementary information available should be included here]. See DOI: 10.1039/x0xx00000x

transported through the tripodal platform, while the principal molecular axis and top –CN moiety are beyond the transport pathway. This behavior was explained by a relatively weak interaction between the gold STM probe and the top –CN moiety of the molecule.[21]

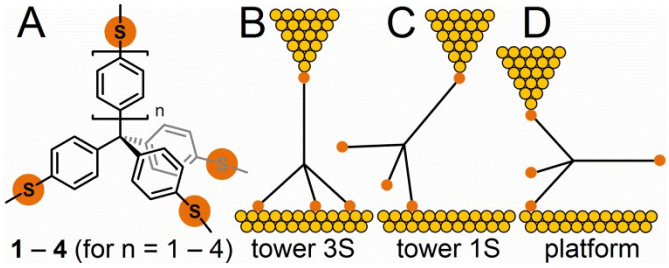

Scheme 1 Chemical structure of investigated compounds **1** to **4** for n = 1 to 4 (A). Theoretically considered tower 3S (B), tower 1S (C) and platform (D) configurations of MJs.

In this work, we aim at investigating the single molecule charge transport through tetraphenylmethane based molecular conductors **1** to **4** containing four thiolate anchoring groups with a possibility of three of them forming one tripodal anchor (see Scheme 1). We are the first to determine the contact conductance value for a tripodal platform and demonstrate favorable tuning of the contact conductance of the anchoring group that leads to an increase of the single molecule conductance by more than one order of magnitude thanks to the involvement of three parallel transport pathways. So far, characteristics of systems involving parallel transport pathways were reported only for molecules with two identical transport channels, observing non-additive conductance behavior in all cases. Xing *et al.*[26] investigated charge transport characteristics of phenylene-ethynylene based molecular conductors terminated with monopodal thiol and bipodal carbodithioate linkers concluding that the dipodal attachment enhances the electronic coupling (contact conductance) of the junction by a factor of five compared to the monopod. Interestingly, Tivanski *et al.*[27] discovered that the conductance of junctions containing biphenyl based conductors capped by the above-mentioned two moieties differs only by ≈35 %. Kiguchi *et al.*[28] devised and investigated molecular conductors based on 5-sulfanylthiophen-2-ylethynyl anchors with either one or two conductance pathways observing that single molecule conductance value of the two derivatives differs by a factor of five. Vazquez *et al.*[29] compared experimental and theoretical single molecule conductance values for molecular conductors with single and double conductance pathway. Positive non-additivity was ascribed to constructive quantum interference in molecules with the doubled backbone. Seth *et al.*[30] designed, investigated and theoretically analyzed single molecule breadboard circuits based on a bis-terpyridine molecule assigning single molecule conductance states to the underlying constituent circuits. Hansen *et al.*[31] used theoretical approach to compare the charge transport in conjugated molecules with simple and multiple connections to electrodes. Magoga and Joachim[32] provided a general analytical solution for the conductance of single molecules composed of parallel transport pathways. They demonstrated that for the conductor with p identical pathways the overall conductance is proportional to p^2 (quadratic superposition law). First example of the constructive quantum interference was reported by Vazquez *et al.*[29] Presented work can put to test this general theory as well.

Experimental

All four compounds **1** to **4** were synthesized as thioacetates to prevent the oxidation of thiolate anchoring groups by atmospheric oxygen. Their synthesis and characterization is given in detail in the Supporting Information (SI).

Single molecule conductance measurements of **1** to **4** were carried out by in-situ STM-BJ technique in mesitylene solvent. Prior to each measurement thioacetates were converted to thiols by the addition of triethylamine. The current response as a function of distance Δz between a gold substrate and probe in the absence and presence of molecules was monitored. Repetitive formation and breaking of the junctions was performed and retraction curves (3000 to 5000 for each molecule) were further analyzed without any data selection. The approach and retraction rate of the probe was 360 and 36 nm.s^{-1}, respectively. The bias voltage between the substrate and probe electrodes was set to 260 mV. Electric current was converted to conductance G using Ohm´s law. Conductance-distance traces for individual compounds were processed statistically to obtain 1D and 2D conductance histograms and the plateau length histograms. The characteristic length of the MJs was calculated as $z_{exp} = \Delta z^* + z_{corr}$, where z_{corr} = 0.4 nm is a snap-back correction and Δz^* is the experimentally obtained molecular plateau length. Detailed description of experimental procedures, STM-BJ setup and data analysis was described previously[15,33]. Further experimental details are given in the SI.

The charge transport in single MJs of investigated compounds was further analyzed theoretically by combining DFT and non-equilibrium Green's function (NEGF) formalism. Theoretical junction conductance value *G* was derived from the value of the transmission function $\tau(\varepsilon_F)$ obtained at the Fermi level of electrodes by Landauer approach using zero-bias approximation[34,35] and applying formula $G = G_0 \times \tau(\varepsilon_F)$[36,37] where G_0 is the conductance quantum equal to 77.5 μS and ε_F is experimentally obtained Fermi energy of gold equal to -5.1 ± 0.1 eV.[38] Theoretical conductance was obtained for various geometrical MJ arrangements, which allowed experimentally obtained single molecule conductance features to be assigned to a particular charge transport pathway through the molecule.[15,21] Theoretical MJ length was obtained as $L = z_{theor} - d_{Au}$, where z_{theor} is the perpendicular distance of planes of two gold electrodes involving centers of surface atoms and d_{Au} = 0.25 nm is the diameter of the gold atom. Further computational details are given in the SI.

Results and discussion

Charge transport characteristics of single MJs of **1** to **4** were obtained by the STM-BJ technique in the solution of respective molecules. For each compound, several thousands of individual junctions were formed and broken between the substrate and the probe. Obtained conductance-distance (G vs. Δz) traces were processed by means of statistical analysis without any data selection.[15] Presented 1D conductance and 2D conductance-distance histograms depict logarithm of junction conductance $\log(G/G_0)$ referenced to the conductance quantum G_0. Results are demonstrated taking the longest compound **4** as the representative of the investigated series (Fig. 1). Characteristics of all four derivatives complemented by their typical individual conductance-distance traces are shown in Figs. S18 to S21 in the SI.

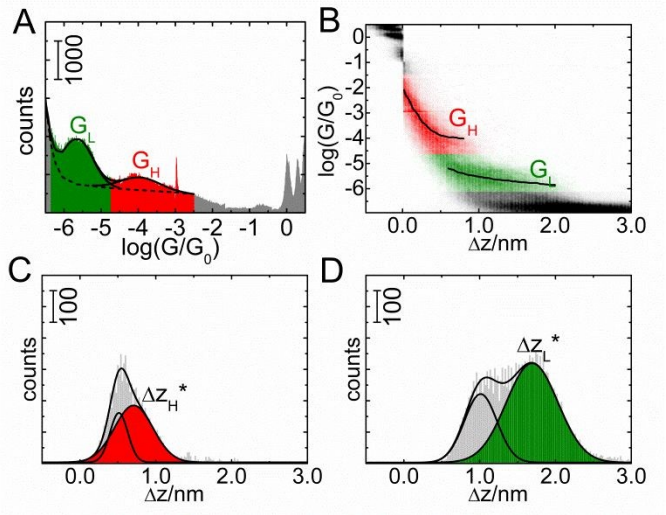

Fig. 1 1D conductance (A) and 2D conductance-distance (B) histogram and plateau length histogram obtained for the G_H(C) and G_L (D) feature shown for the compound **4**.

Maxima observed in 1D conductance (Fig. 1A) and horizontal plateaus observed in 2D conductance-distance (Fig. 1B) histograms at $\log(G/G_0) \geq 0$ reflect the existence of nanojunctions involving one or few gold atoms formed in the early stage of the junction evolution.[39] Breaking gold nanocontacts upon pulling electrodes apart manifests itself as a sudden drop in the junction conductance value by two to three orders of magnitude. The presence of a molecule between electrodes gives rise to further feature(s) in the range of measurable conductance values. This range is limited by the onset of the instrumental noise level at $\log(G/G_0) \sim$ -6.5 for our STM-BJ setup. For molecule **4** in Fig. 1, two molecular features centered at $\log(G_H/G_0)$ = -3.9 ± 0.6 (red) and $\log(G_L/G_0)$ = -5.6 ± 0.5 (green) were observed. Two values were obtained as maxima of the best baseline-corrected double Gaussian fit (Fig. 1A) and are further regarded as single molecule conductance values of **4**. Master curves of features G_H and G_L were obtained by evaluating the weighted average of counts at $\log(G/G_0)$ values as a function of Δz (black curves in Fig. 1B) and depict the characteristic evolution of MJs. Histograms constructed for molecules **2** and **3** (see Figs. S19 and S20 of the SI) show G_H or G_L features similar to **4** while a single feature G_H is observed for the shortest molecule **1** (see Fig. S18 of the SI).

Plateau length distributions (Fig. 1C and 1D) were constructed by plotting horizontal cross-section through data-points in the 2D histogram negative to G_H and G_L features. Both distributions show two maxima originating due to through solvent tunneling event (not considered further) and formation of MJs (red/green maximum). The characteristic MJ length Δz^* obtained by data fitting amounts to Δz_H^* = 0.7 nm (red) and Δz_L^* = 1.7 nm (green). These two values were used further to obtain experimental MJ length z_{exp}^H and z_{exp}^L (see Experimental part for details).

Fig. 2 summarizes experimentally-obtained values of single molecule conductance $\log(G_H/G_0)$ (A), $\log(G_L/G_0)$ (B) and MJ lengths z_{exp}^H (C) and z_{exp}^L (D) shown as filled symbols.

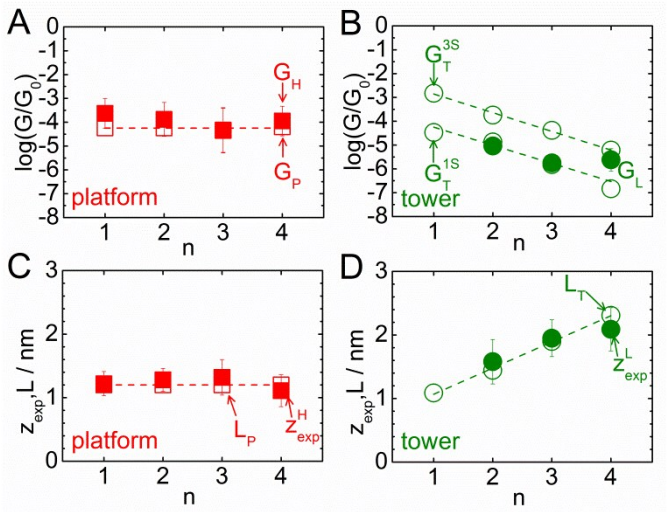

Fig. 2 Experimentally obtained (filled symbols) and theoretically predicted (empty symbols) values of conductance (A, B) and length (C, D) of MJs as a function of n.

The existence of two conductance features G_H and G_L for **2** to **4** suggests that the charge transport through their single molecules involves more than one pathway. The DFT/NEGF theoretical approach was applied to determine single molecule conductance values of MJs with varied transport pathways and geometries aiming at finding most probable configurations of MJs for experimental G_H and G_L features. In the theoretical analysis, the principal molecular axis was either considered as involved ("tower" configurations) or omitted ("platform" configurations) from the pathway. Tower configurations differ from each other in the number of covalent attachments between the platform and the electrode, considering either one (1S, Scheme 1C) or three (3S, Scheme 1B) thiolate-gold bonds. The tripod geometry comprising two thiolate-gold bonds is not computationally accessible due to restrictions on the charge neutrality of the system. Subtraction of three hydrogen radicals and formation of three gold-thiolate bonds including two from the tripod and one from the oligophenylene molecular wire would yield radical species. Experimentally this is not the case. Even though the theoretical analysis can deal with this problem by making adjustments to the MJ model to provide a closed-shell system, we did not

follow this path. For this reason we did not treat theoretically 2S tripodal configuration. Optimized geometries of the 1S and 3S type of tower MJ configurations of **4** are shown in Fig. 3B and 3A. For platform configurations, the attachment of one thiolate-gold bond to each electrode is considered (Scheme 1D) and the distance between electrodes L_P (see Experimental for its exact definition) is left as a variable changing from 0.8 nm to 1.3 nm. Figure 3D shows the optimized geometry of the platform configuration of **4** (L_P= 1.0 nm), while Fig. 3E shows an example of the MJ geometry with elongated electrode distance (L_P= 1.2 nm). Transmission functions $\tau(\varepsilon)$ obtained for varied geometries of tower and platform MJ configurations of **4** are plotted in Fig. 3C and 3F. Figure 3F shows changes in the transmission function $\tau(\varepsilon)$ as the length of the platform MJ configuration increases. Figures S27 and S28 in the SI show a comprehensive list of transmission functions obtained for all MJ configurations and geometries of all four derivatives studied.

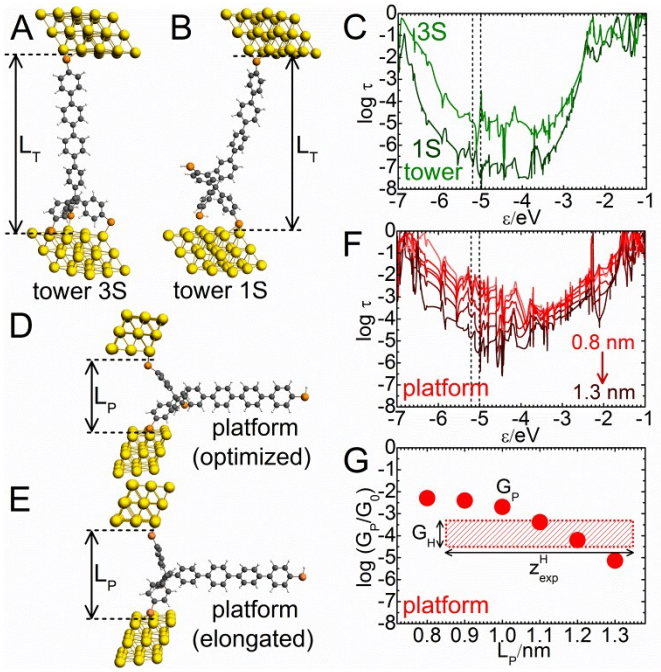

Fig. 3 Geometries of tower (A,B) and platform (D,E) configurations; transmission functions of tower (C) and platform (F) MJ configurations of **4**. Panel G shows theoretical G_P values for platform configuration as a function of L_P (filled circles) and comparison with experimental G_H and z^H_{exp}values (dashed rectangle).

Figure 3G compares theoretical $\log(G_P/G_0)$ values of **4** as a function of L_P (filled circles representing *G* values calculated from the transmission functions shown in Fig. 3F) with the experimental value of $\log(G_H/G_0)$ = -3.9 ± 0.6 of **4** (dashed rectangle) suggesting that a good agreement is obtained for L_P = 1.2 nm. This indicates that the experimentally achieved G_H state of MJs originates due to platform configurations with slightly elongated electrode distance. The same conclusion was arrived at for all four derivatives (Fig. 2A) and is further corroborated by a perfect match between theoretically predicted (L_P) and experimentally obtained (z^H_{exp}) MJ length values (Fig. 2C). A perfect agreement between experimental $\log(G_L/G_0)$ and theoretical $\log(G_T^{1S}/G_0)$ values of **2** and **3** (Fig. 2B) indicates that the G_L state of MJs involves tower configurations with the tripod attached to the electrode by one thiolate-gold bond (Scheme 1C). On the contrary, a good match between experimental $\log(G_L/G_0)$ and theoretical $\log(G_T^{3S}/G_0)$ conductance values observed for **4** confirms the attachment of the tripod to the electrode by all three thiolate-gold bonds (Scheme 1B and Fig. 3A).

It should be emphasized that for tower configurations, the comparison of experimental z^L_{exp} and theoretical L_T lengths of MJs cannot differentiate between 1S and 3S geometries as the two arrangements have virtually the same MJ length (compare L_T^{1S} and L_T^{3S} values in Table S9). The assignment of the geometry in the tower MJ configuration thus has to rely solely on the comparison of single molecule conductance values. Importantly, an excellent overall agreement between z^L_{exp} and L_T values and the linear proportionality of both characteristics to n (Fig. 2D) clearly demonstrates that tower MJs reach fully elongated geometries (Fig. 3A and 3B) in the G_L state of MJs as anticipated for thiolate anchoring moieties.[40]

The results of the DFT/NEGF analysis performed for 1S and 3S geometries of tower MJ configurations of **1** to **4** may be further used to quantify the coupling between the tripod and the gold electrode by comparing contact conductance (G_c) values for these two geometries. Assuming tunneling as operating charge transport mechanism, the conductance of a molecule is given by $G_T = G_c e^{-\beta L_T}$, where β is a parameter describing the attenuation of the electric conductance through the molecular backbone (oligo-1,4-phenylene in this work). The values of G_c and β may be extracted by fitting the dependence of $\ln G_T$ on L_T (see Fig. S29 in the SI). The contact conductance G_c values obtained for 1S and 3S geometries of tower MJs amount to G_C^{1S}= 0.39 μS and G_C^{3S}= 8.7 μS, leading to the ratio G_C^{3S}/G_C^{1S}= 22. This ratio is higher than the ratio G_C^{2S}/G_C^{1S} = 5 extrapolated from conductance values of oligo(phenylene-ethynylene) wires terminated with carbodithiol (2S) and thiol (1S) anchoring groups reported by Xing *et al.*[26] thus confirming better charge transport properties of tripod compared to bipodal and monopodal anchors.

Single molecule anchoring by all three thiolate groups of the tripod leads to a significant increase of the conductance upon the formation of additional two sulfur-gold bonds (Fig. 3A to 3C). The obtained ratio of 22 is much higher than that predicted theoretically for three identical parallel charge transport pathways (p = 3) by the quadratic superposition law (p^2= 9) and indeed confirms the constructive quantum interference.[32]

The found values of β^{3S} = 4.2 ± 0.1 nm^{-1} and β^{1S} = 4.4 ± 0.4 nm^{-1} for 1S and 3S tower geometries indicate that the coupling between the tetraphenylmethane tripod and the electrode has virtually no impact on the intrinsic electric conduction through the oligo-1,4-phenylene backbone. The two values of β fall within the range of values reported in the literature for oligo-1,4-phenylene based molecular wires (3.5 – 5.0 nm^{-1}).[41]

Additionally, we have a unique opportunity to compare the experimental conductance of G_L state for oligo-1,4-phenylene molecular wires that contain the tetraphenylmethane tripod with thiolate anchors either in the *para* (molecule **4** of this

paper) or in the *meta* position (molecule **4** reported in Kolivoška *et al.*[22]) Experimental single molecule conductance for *para* connected molecule **4** is G_L^{para}= 2.0 × 10^{-4} μS and that for *meta* is G_L^{meta} = 1.2 × 10^{-4} μS, respectively. Theoretical ln G_T^{3S} values for *para* and *meta* derivatives **1** to **4** were plotted against theoretical L_T^{3S} values (see Fig. S30 in the SI) and further corroborated our experimental finding giving the higher contact conductance value G_C^{3S} for *para* compared to *meta* connected tripod. The single molecule conductance ratio G_L^{para}/G_L^{meta} = 1.67 obtained for **4** in this work is higher than the ratio obtained for *para*- and *meta*-benzenedithiol (BDT) $G_{BDT}^{para}/G_{BDT}^{meta}$= 1.25 reported in the literature.[42] The observed difference is most likely due to the involvement of three thiolate anchors in the covalent attachment of the tetraphenylmethane tripod to the electrode. Higher value of G_L^{para} compared to G_L^{meta} is consistent with theoretical predictions considering quantum interference effects in substituted benzene cores.[43]

We have demonstrated that the experimentally observed transition in the tower MJ geometry of **2** and **3** on one hand and **4** on the other hand occurs due to a change in the number of covalent bonds with the electrode. Importantly, the change in the molecular design represented by the length of oligo-1,4-phenylene backbone (1) allows tuning contact conductance of the anchoring platform and (2) leads to the formation of favorable directional arrangement of the tripod on the gold surface (Fig. 3A) that involves three thiolate-gold covalent bonds. In such configuration the principal molecular axis is directed towards the top of the molecular assembly and can potentially carry molecular electronic functional groups to be addressed by external stimuli such as light, a scanning probe or species dissolved in the solution bulk.

Conclusions

Experimental STM-BJ approach and computational DFT/NEGF analysis were employed to investigate the single molecule charge transport in a series of conductors with the tetraphenylmethane tripodal platform supporting the wire composed of one to four 1,4-phenylene repeating units (compounds **1** to **4**). Derivatives **2** to **4** show two distinct experimental single molecule features G_H and G_L unambiguously assigned to the theoretically modelled charge transport pathway solely through the tripod (platform configuration) and the entire molecule involving the wire (tower configuration), respectively.

A detailed theoretical configurational analysis of G_L feature revealed that for derivatives **2** and **3** the tripodal platform is attached to the electrode by one thiolate anchor (1S) while all three sulfur atoms (3S) are contacting the electrode in the case of the derivative **4**.

Theoretically obtained $G_T^{1S}$and G_T^{3S}data sets further provided the contact conductance of the tripodal platform G_c^{1S} and G_c^{3S}. The values of β are nearly independent of the contact geometry, while a high ratio of G_T^{3S}/G_T^{1S}equal to 22 was found. This is much higher value than that predicted by the quadratic superposition law.[32] We also demonstrated that the contact geometry of the tripod is controlled by the molecular length. The geometry achieved for the derivative **4** allows an enhanced electronic communication and well-defined directional self-assembly of molecules on the electrode. The conductance of **4** is even higher than that of a molecule anchored to the gold electrode by the tetraphenylmethane tripod containing thiols in *meta* position.[22] The molecular architecture of **4** may thus be employed as a well-defined platform to support functional components for molecular electronic applications.

Conflicts of interest

There are no conflicts to declare.

Acknowledgements

The financial support by the Czech Science Foundation (18-14990S, 18-04682S), Czech Academy of Sciences (MTA-16-02, RVO: 61388955), Hungarian Academy of Sciences OTKA (NN 128168), Baden-Württemberg Stiftung (Functional Nano-structures) and the Helmholtz Research Program (Science and Technology of Nanosystems, "STN").

Notes and references

1 M. Valášek, M. Lindner and M. Mayor, *Beilstein J. Nanotechnol.*, 2016, **7**, 374.
2 M. Valášek and M. Mayor, *Chem. Eur. J.*, 2017, **23**, 13538.
3 Z. Wei, X. Wang, A. Borges, M. Santella, T. Li, J. K. Sørensen, M. Vanin, W. Hu, Y. Liu, J. Ulstrup, G. C. Solomon, Q. Chi, T. Bjørnholm, K. Nørgaard and B. W. Laursen, *Langmuir*, 2014, **30**, 14868.
4 N. Hauptmann, L. Gross, K. Buchmann, K. Scheil, C. Schütt, F. L. Otte, R. Herges, C. Herrmann and R. Berndt, *New J. Phys.*, 2015, **17**, 013012.
5 S. Lemke, S. Ulrich, F. Claussen, A. Bloedorn, U. Jung, R. Herges and O. M. Magnussen *Surf. Sci.*, 2015, **632**, 71.
6 S. Kuhn, U. Jung, S. Ulrich, R. Herges and O. Magnussen, *Chem. Commun.*, 2011, **47**, 8880.
7 B. Singhana, A. C. Jamison, J. Hoang and T. R. Lee, *Langmuir*, 2013, **29**, 14108.
8 S. Katano, Y. Kim, T. Kitagawa and M. Kawai, *Phys. Chem. Chem. Phys.*, 2013, **15**, 14229.
9 T. Kitagawa, Y. Idomoto, H. Matsubara, D. Hobara, T. Kakiuchi, T. Okazaki and K. Komatsu, *J. Org. Chem.*, 2006, **71**, 1362.
10 T. Kitagawa, H. Matsubara, K. Komatsu, K. Hirai, T. Okazaki and T. Hase, *Langmuir*, 2013, **29**, 4275.
11 S. U. Lee, H. Mizuseki and Y. Kawazoe, *Phys. Chem. Chem. Phys.*, 2010, **12**, 11763.
12 K. Scheil, T. G. Gopakumar, J. Bahrenburg, F. Temps, R. J. Maurer, K. Reuter and R. Berndt, *J. Phys. Chem. Lett.*, 2016, **7**, 2080.
13 M. Valášek, K. Edelmann, L. Gerhard, O. Fuhr, M. Lukas and M. Mayor, *J. Org. Chem.*, 2014, **79**, 7342.
14 M. A. Karimi, S. G. Bahoosh, M. Valášek, M. Bürkle, M. Mayor, F. Pauly and E. Scheer, *Nanoscale*, 2016, **8**, 10582.

15 J. Šebera, V. Kolivoška, M. Valášek, J. Gasior, R. Sokolová, G. Mészáros, W. Hong, M. Mayor and M. Hromadová, *J. Phys. Chem. C*, 2017, **121**, 12885.
16 L. Gerhard, K. Edelmann, J. Homberg, M. Valášek, S. G. Bahoosh, M. Lukas, F. Pauly, M. Mayor and W. Wulfhekel, *Nat. Commun.*, 2017, **8**, 14672.
17 M. Lindner, M. Valášek, M. Mayor, T. Frauhammer, W. Wulfhekel and L. Gerhard, *Angew. Chem. Int. Ed.*, 2017, **56**, 8290.
18 M. Lindner, M. Valášek, J. Homberg, K. Edelmann, L. Gerhard, W. Wulfhekel, O. Fuhr, T. Wächter, M. Zharnikov, V. Kolivoška, L. Pospíšil, G. Mészáros, M. Hromadová and M. Mayor, *Chem. Eur. J.*, 2016, **22**, 13218.
19 Y. Ie, T. Hirose, H. Nakamura, M. Kiguchi, N. Takagi, M. Kawai and Y. Aso, *J. Am. Chem. Soc.*, 2011, **133**, 3014.
20 Y. Ie, K. Tanaka, A. Tashiro, S. K. Lee, H. R. Testai, R. Yamada, H. Tada and Y. Aso, *J. Phys. Chem. Lett.*, 2015, **6**, 3754.
21 T. Sebechlebská, J. Šebera, V. Kolivoška, M. Lindner, J. Gasior, G. Mészáros, M. Valášek, M. Mayor and M. Hromadová, *Electrochim. Acta*, 2017, **258**, 1191.
22 V. Kolivoška, J. Šebera, T. Sebechlebská, M. Lindner, J. Gasior, G. Mészáros, M. Mayor, M. Valášek and M. Hromadová, *Chem. Commun.*, 2019, **55**, 3351.
23 S. Ramachandra, K. C. Schuermann, F. Edafe, P. Belser, Ch. A. Nijhuis, W. F. Reus, G. M. Whitesides and L. De Cola, *Inorg. Chem.*, 2011, **50**, 1581.
24 R. Sakamoto, Y. Ohirabaru, R. Matsuoka, H. Maeda, S. Katagiri and H. Nishihara, *Chem. Commun.*, 2013, **49**, 7108.
25 B. Xu and N. J. Tao, *Science*, 2003, **301**, 1221.
26 Y. Xing, T.-H. Park, R. Venkatramani, S. Keinan, D. N. Beratan, M. J. Therien and E. Borguet, *J. Am. Chem. Soc.*, 2010, **132**, 7946.
27 A. V. Tivanski, Y. He, E. Borguet, H. Liu, G. C. Walker, D. H. and Waldeck, *J. Phys. Chem. B*, 2005, **109**, 5398.
28 M. Kiguchi, Y. Takahashi, S. Fujii, M. Takase, T. Narita, M. Iyoda, M. Horikawa, Y. Naitoh and H. Nakamura, *J. Phys. Chem. C*, 2014, **118**, 5275.
29 H. Vazquez, R. Skouta, S. Schneebeli, M. Kamenetska, R. Breslow, L. Venkataraman and M. S. Hybertsen, *Nat. Nanotechnol.*, 2012, **7**, 663.
30 C. Seth, V. Kaliginedi, S. Suravarapu, D. Reber,W. Hong, T. Wandlowski, F. Lafolet, P. Broekmann, G. Royal and R. Venkatramani, *Chem. Sci.*, 2017, **8**, 1576.
31 T. Hansen and G. C. Solomon, *J. Phys. Chem. C*, 2016, **120**, 6295.
32 M. Magoga and C. Joachim, *Phys. Rev. B*, 1999, **59**, 16011.
33 J. Šebera, T. Sebechlebská, Š. Nováková Lachmanová, J. Gasior, P. Moreno Garcia, G. Mészáros, M. Valášek, V. Kolivoška and M. Hromadová, *Electrochim. Acta*, 2019, **301**, 267.
34 L. Rincon-Garcia, C. Evangeli, G. Rubio-Bollinger and N. Agrait, *Chem. Soc. Rev.*, 2016, **45**, 4285.
35 Š. Nováková Lachmanová, J. Šebera, V. Kolivoška, J. Gasior, G. Mészáros, G. Dupeyre, P. P. Lainé and M. Hromadová, *Electrochim. Acta*, 2018, **264**, 301.
36 J. C. Cuevas and E. Scheer, *Molecular Electronics: An Introduction to Theory and Experiment*, World Scientific, New Jersey, USA, 2010.
37 M. Di Ventra, *Electrical Transport in Nanoscale Systems*, Cambridge University Press, Cambridge, UK, 2008.
38 S. C. Veenstra, U. Stalmach, V. V. Krasnikov, G. Hadziioannoua, H. T. Jonkman, A. Heeres and G. A. Sawatzky, *Appl. Phys. Lett.*, 2000, **76**, 2253.
39 N. Agrait, J. G. Rodrigo and S. Vieira, *Phys. Rev. B*, 1993, **47**, 12345.
40 P. Moreno-García, M. Gulcur, D. Z. Manrique, T. Pope, W. Hong, V. Kaliginedi, C. Huang, A. S. Batsanov, M. R. Bryce, C. Lambert and T. Wandlowski, *J. Am. Chem. Soc.*, 2013, **135**, 12228.
41 V. Kaliginedi, A. V. Rudnev, P. Moreno-Garcia, M. Baghernejad, C. Huang, W. Hong and T. Wandlowski, *Phys. Chem. Chem. Phys.*, 2014, **16**, 23529.
42 M. Kiguchi, H. Nakamura, Y. Takahashi, T. Takahashi and T. Ohto, *J. Phys. Chem. C*, 2010, **114**, 22254.
43 T. Markussen, R. Stadler and K. S. Thygesen, *Nano Lett.*, 2010, **10**, 4260.

Molecular design allows tuning of the contact conductance of anchoring groups in single molecule junction.